UTE MRI versus Dual-Energy CT for Imaging Different Kidney Stones Types

El-Sayed H. Ibrahim[1,2], Robert Pooley[2], Mellena Bridges[2], Joseph Cernigliaro[2], James Williams[3], and William Haley[2]
[1]University of Michigan, Ann Arbor, MI, United States, [2]Mayo Clinic, Jacksonville, FL, United States, [3]Indiana Unicersity, IN, United States

INTRODUCTION: Kidney stones are very common, painful, recurrent, increasing in incidence, and associated with co-morbid conditions and high cost [1]. Computed Tomography (CT) has been established as the method of choice for kidney stone imaging with 90-100% sensitivity [2]. Further, the recent introduction of dual-energy CT (DECT) scanners added the capability of identifying uric acid (UA) from non-UA stones [3]. However, an important drawback of CT scanning is the associated ionizing radiation exposure, especially in vulnerable patients including children and pregnant women. MRI, which averts radiation concerns, is a potential alternative to CT imaging of kidney stone formers, especially among the most vulnerable patients; however, traditional MRI is insensitive to imaging kidney stones. With the advent of ultra-short echo time (UTE) MRI sequences, adequate imaging of kidney stones becomes possible [4]. The purpose of this work is to compare MRI versus DECT imaging of 114 kidney stones, representing different stone types and sizes, in phantom experiments using different surrounding materials and scan setups.

METHODS: One hundred and fourteen kidney stones, passed or extracted from patients, were obtained. The stone types (count) are as follows: apatite (15), brushite (14), calcium oxalate monohydrate (COM, 15), calcium oxalate dehydrate (COD, 15), cystine (16), struvite (15), uric acid (UA, 13), and mixed (8), based on micro CT analysis. The stones' size ranged from 2 to 10 mm. An agarose phantom (Figure 1(a,b)) was created as follows. One hundred and fourteen 5-ml tubes were filled with an agarose-based material, created by dissolving 0.5% agarose in distilled water and doping the mixture with 0.085 milli-molar of $MnCl_2$ to create a gel-like material with T1 and T2 time constants similar to those in the kidney [5]. Each kidney stone was inserted inside a separate tube. The agarose phantom was imaged using DECT on a Siemens Flash scanner using renal stone imaging protocols with the following parameters: tube voltages / reference effective tube current-time product = 80 kVp / 419 mAs and 140kVp / 162 mAs; collimation= 32×0.6 mm; and pitch= 0.7. The images were postprocessed to create material-specific chromatic image, based on the dual-energy ratio (DER) between the two images acquired with different kVp's, with 1.0 mm slice thickness and using D30f convolution kernel.

Following the CT scan, the agarose phantom was imaged on a Siemens Skyra 3T MRI scanner using a bird-cage head coil. The point-wise encoding time reduction with radial acquisition (PETRA) UTE pulse sequence was used for imaging the stones [6] with the following imaging parameters: flip angle = 6°; repetition time (TR) = 25 ms; first echo time (TE1) = 0.07 ms; second echo time (TE2) = 15 ms; slice thickness = 0.79 mm; field of view (FOV) = 280×280 mm^2; matrix = 352×352; number of radials = 2500; bandwidth = 1895 Hz/pixel; number of averages = 1; and scan time = 3:21 min. The stones were also imaged with different TE's ranging from 0.1 ms to 15 ms to measure their T2 time constants using exponential fitting with in-house software written in Matlab. It should be noted that the stones' T1values have been previously shown to be close for different stone types [4]. The agarose phantom was then imaged again with MRI using the same protocol and on the same scanner as described above, except that the head coil was replaced by a body surface coil to examine scan-rescan reproducibility using the body surface coil, which is typically used for in vivo abdominal / pelvic imaging. After the second MRI scan, the stones were removed from the agarose-filled tubes, washed, and inserted in other tubes filled with urine to create a urine phantom, as shown in Figure 1(c). The urine phantom was then imaged with the same protocols and on the same scanners described above using only the body surface coil in MRI. Statistical *t* test was conducted to examine the differences in T2 measurements from different MRI scans and for different stone types.

RESULTS: All stones were visible in different CT and MRI scans. Figure 2 shows sample stones of different types, along with the resulting MRI and DECT images. DECT allowed for identifying the UA stones (colored in red) from all other stones (colored in blue). Table 1 shows the DER values for different stone types, as well as the calculated T2 values for different stone types and from different MRI scans. DER was significantly different between UA and non-UA stones. Statistical analysis showed insignificant ($P > 0.01$) differences in T2 values between different scans or stone types.

DISCUSSION: The results show the capability of MRI for imaging kidney stones of different types and sizes with high resolution in a relatively short scan time. The images show the shape of the stone and are comparable to those obtained from the gold standard CT images. MRI measurements were reproducible regardless of the receiver coil used for data acquisition or the material surrounding the stone. Although DECT is capable of differentiating between UA and non-UA stones based on DER, MRI showed insignificant differences between different types, which may be improved using multi-parametric MR imaging with different contrasts, especially with ongoing advances in the MRI scanners' hardware and pulse sequences capabilities. In summary, the capability of MRI of visualizing kidney stones of all types and different sizes is promising for in vivo imaging in the future. Future work includes using the developed technique for in vivo imaging.

CONCLUSIONS: MRI is capable of reliably imaging kidney stones of different types and sizes with results comparable to those from CT. Therefore, MRI could provide a valuable alternative for imaging vulnerable patients who have higher sensitivity to ionizing radiation.

REFERENCES: [1] Prim Care 35:369-91; [2] AJR 172:1485-90; [3] Radiology 250:813-20; [4] Acad Radiol 19:1566-72; [5] Hemogl 36:343-61; [6] MRM 67:510-8.

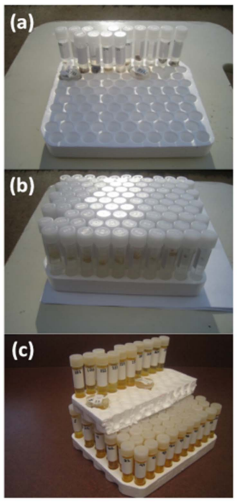

Figure 1. Agarose phantom (a,b), and urine phantom (c).

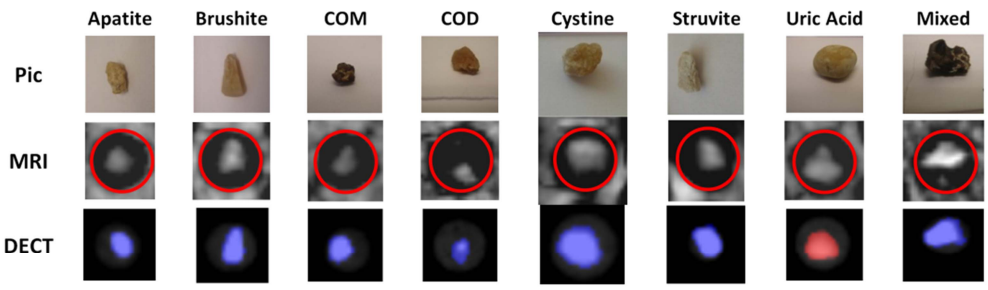

Figure 2. Different kidney stones (top) imaged with UTE MRI (middle) and DECT (bottom).

Table 1. CT dual-energy ratio (DER) and MRI T2 values. Ag = agarose; Ur = urine; B = body coil; H = head coil.

	Apatite	Brushite	COM	COD	Cystine	Struvite	UA	Mixed
DER	1.97±0.16	1.84±0.09	1.89±0.11	2.03±0.20	1.53±0.10	1.75±0.12	1.01±0.09	1.57±0.42
T2, Ag, B	4.4±1.2	4.2±0.8	6.6±1.8	5.2±1.2	6.1±1.9	4.8±1.9	6.0±2.7	6.2±2.7
T2, Ag, H	4.8±2.5	4.2±0.9	5.9±1.5	5.3±1.4	5.6±2.4	5.4±2.7	6.2±2.8	5.9±2.3
T2, Ur, H	6.2±1.7	5.0±0.8	6.6±1.5	6.0±1.3	6.0±1.3	5.3±1.7	7.5±2.1	6.5±1.3